COMPUTATIONAL MECHANICS 2023
38th conference with international participation
Srní
October 23 - 25, 2023

Modelling of bowed fuel assemblies vibration in mixed reactor core

V. Zeman[a], Z. Hlaváč[a], Š. Dyk[a]

[a] *NTIS – New Technologies for the Information Society, Faculty of Applied Sciences, University of West Bohemia, Univerzitní 8, 301 00 Plzeň, Czech Republic*

1. Introduction

A pressurized-water reactor core includes a large number of fuel assemblies (FAs) of the same or different types. During the reactor operation, FAs can be statically deformed in the lateral and/or torsional direction. This phenomenon is called FA bow [1, 3]. This contribution is focused on the mathematical modelling of the vibration of two different types bowed FAs in interaction. The aim of the modelling is a description of changes in FA's dynamic behaviour in the case of contacting FAs in the mixed reactor core.

2. Concept of the modelling

The presented method is based on the two-stage modelling concept, whose scheme is depicted in Fig. 1. The *first-stage model* represents the global nonlinear model of the VVER 1000 type reactor. The original reactor model [4, 5] with homogeneous reactor core (HCR) was modified

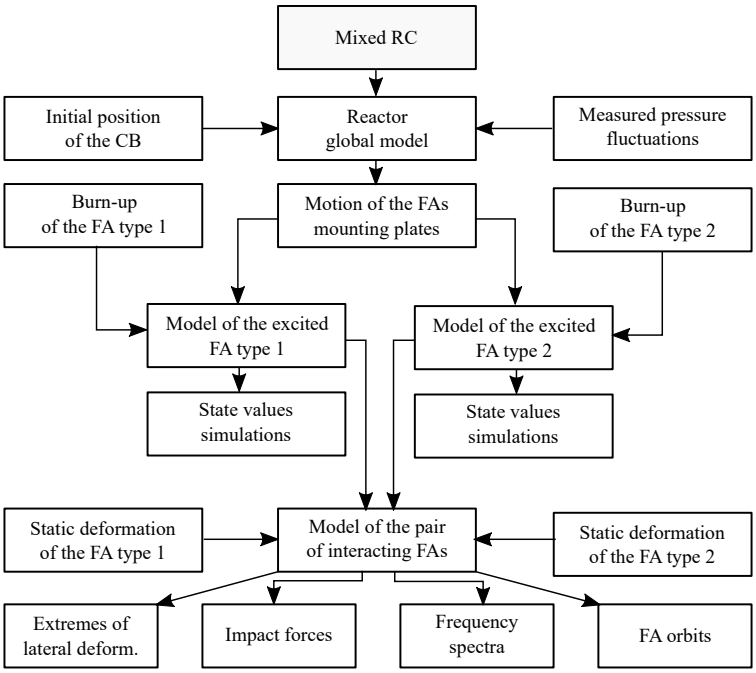

Fig. 1. Scheme of the two-stage modelling of the FAs vibration in the mixed reactor core (FA = fuel assembly, RC = reactor core, CB = core barrel)

for the mixed reactor core (MCR) containing FAs of two types. This new reactor model was created under the following assumptions:

1. FAs of both types were modelled as 1D beam-type continua based on the modal values of their detailed models.
2. An excitation of the reactor is based on time-series of the pressure fluctuations measured at the coolant inlet to reactor core [2] under standard operation.
3. Motion of the FAs mounting plates investigated on the global reactor model is the source of the FAs kinematic excitation.

In the *second-stage model*, both FA types are modelled more in detail (see Fig. 15 in [1]). The load-bearing skeleton (S) is made of six angles rigidly fixed with eight (type 1) or twelve (type 2) spacer grids. The spacer grids together with the rims and parts of the angles in the rim width are modelled as rigid hexagonal plates. Other FA components – fuel claddings (C), fuel pellets (FP) stacks, guide thimbles (GT) and central tube (CT) – are modelled as a beam-type continua. Interaction between the neighbouring FAs can occur due to their static deformations and kinematics excitation by mounting plates movement.

3. Mathematical model of the pair FAs inside the mixed reactor core

Considering a pair of neighbouring FAs composed of statically deformed FA_1 (type 1) and geometrically ideal FA_2 (type 2). Contact of the FAs can be assumed in the area of the vertices of the skeleton angles on the contact line (Fig. 2).

Let us denote normal contact forces $\bar{N}_{1,2}$ and $\bar{\bar{N}}_{1,2}$ at the contact line between FA_1 and FA_2. These forces can be written in the form

$$\begin{aligned} \bar{N}_{1,2} &= k_C(\bar{n}_{1,2} - \delta)H(\bar{n}_{1,2} - \delta), \\ \bar{\bar{N}}_{1,2} &= k_C(\bar{\bar{n}}_{1,2} - \delta)H(\bar{n}_{1,2} - \delta), \end{aligned} \tag{1}$$

where k_C is the contact stiffness between two skeleton angles and δ is the nominal clearance between FAs in the normal $n_{1,2}$ direction. Relative displacements $\bar{n}_{1,2}$ and $\bar{\bar{n}}_{1,2}$ of the vertices of FA_1 angles with respect to the vertices of FA_2 angles in the direction of normal $n_{1,2}$ are expressed using FAs generalized coordinates and static deformations parameters. A necessary condition for the activation of any normal contact forces is a positive argument of the Heaviside function H in (1).

Activated normal contact forces $N_{1,2} \in \{\bar{N}_{1,2}, \bar{\bar{N}}_{1,2}\}$ generate tangential an axial friction forces (see Fig. 2)

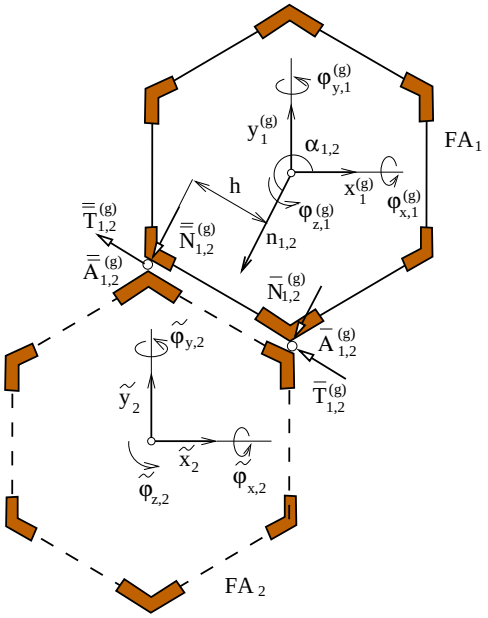

Fig. 2. Contact forces between FAs

$$T_{1,2} = f(c_{1,2})N_{1,2}\frac{c_{1,2,t}}{c_{1,2}}, \qquad A_{1,2} = f(c_{1,2})N_{1,2}\frac{c_{1,2,ax}}{c_{1,2}}. \tag{2}$$

The friction coefficient $f(c_{1,2})$ depends on the absolute sliding velocity $c_{1,2}$ between the vertices of the contacting angles [1]. The tangential sliding velocity $c_{1,2,t}$ is common to both contact points. The axial sliding velocity $c_{1,2,ax}$ in contact points at the contact line is given by the different expressions according to the mutual position of interacting FAs.

The mathematical model of a pair of neighboring FAs of different type can be written in the form

$$\begin{bmatrix} \boldsymbol{M}_1 & \mathbf{0} \\ \mathbf{0} & \boldsymbol{M}_2 \end{bmatrix}\begin{bmatrix} \ddot{\boldsymbol{q}}_1 \\ \ddot{\boldsymbol{q}}_2 \end{bmatrix}+\begin{bmatrix} \boldsymbol{B}_1 & \mathbf{0} \\ \mathbf{0} & \boldsymbol{B}_2 \end{bmatrix}\begin{bmatrix} \dot{\boldsymbol{q}}_1 \\ \dot{\boldsymbol{q}}_2 \end{bmatrix}+\begin{bmatrix} \boldsymbol{K}_1 & \mathbf{0} \\ \mathbf{0} & \boldsymbol{K}_2 \end{bmatrix}\begin{bmatrix} \boldsymbol{q}_1 \\ \boldsymbol{q}_2 \end{bmatrix}=\begin{bmatrix} \boldsymbol{f}_1^{KE}(t) \\ \boldsymbol{f}_2^{KE}(t) \end{bmatrix}+\begin{bmatrix} \boldsymbol{f}_{2,1}^{C} \\ \boldsymbol{f}_{1,2}^{C} \end{bmatrix}, \quad (3)$$

where $\boldsymbol{M}_j$, $\boldsymbol{B}_j$, $\boldsymbol{K}_j$, $j = 1, 2$ are the mass, damping, and stiffness square matrices of non-interacting FAs of order n_j. The kinematic excitation vectors $\boldsymbol{f}_j^{KE}(t)$, $j = 1, 2$ differ in the structure of FA types and in coordinates describing the position in the MRC. The vectors of contact forces $\boldsymbol{f}_{2,1}^{C}$, $\boldsymbol{f}_{1,2}^{C}$ between FAs are expressed by means of the normal and friction forces in (1) and (2). The dimension of global vector $[\boldsymbol{q}_1^T, \boldsymbol{q}_2^T]^T$ of generalized coordinates is way too large for nonlinear simulations in the time domain. Therefore, the modal reduction $\boldsymbol{q}_j = {}^m\boldsymbol{V}_j\boldsymbol{x}_j$, $j = 1, 2$ with modal submatrices ${}^m\boldsymbol{V}_j \in R^{n_j,m_j}$, $m_j < n_j$ of the undamped non-interacting FA$_j$ is used. The matrices ${}^m\boldsymbol{V}_j$ meet the conditions of orthonormality

$${}^m\boldsymbol{V}_j^T\boldsymbol{M}_j\,{}^m\boldsymbol{V}_j = \boldsymbol{I}_j,\ {}^m\boldsymbol{V}_j^T\boldsymbol{K}_j\,{}^m\boldsymbol{V}_j = {}^m\boldsymbol{\Lambda}_j,\ j = 1, 2\,, \quad (4)$$

where $\boldsymbol{I}_j$ are the identity matrices of order m_j and ${}^m\boldsymbol{\Lambda}_j \in R^{m_j,m_j}$ are the diagonal spectral submatrices composed of FA$_j$ eigenfrequencies squares. Model (3) can be transformed into the form

$$\begin{bmatrix} \ddot{\boldsymbol{x}}_1 \\ \ddot{\boldsymbol{x}}_2 \end{bmatrix}+\begin{bmatrix} \boldsymbol{D}_1 & \mathbf{0} \\ \mathbf{0} & \boldsymbol{D}_2 \end{bmatrix}\begin{bmatrix} \dot{\boldsymbol{x}}_1 \\ \dot{\boldsymbol{x}}_2 \end{bmatrix}+\begin{bmatrix} {}^m\boldsymbol{\Lambda}_1 & \mathbf{0} \\ \mathbf{0} & {}^m\boldsymbol{\Lambda}_2 \end{bmatrix}\begin{bmatrix} \boldsymbol{x}_1 \\ \boldsymbol{x}_2 \end{bmatrix}=\begin{bmatrix} {}^m\boldsymbol{V}_1^T & \mathbf{0} \\ \mathbf{0} & {}^m\boldsymbol{V}_2^T \end{bmatrix}\begin{bmatrix} \boldsymbol{f}_1^{KE}(t)+\boldsymbol{f}_{2,1}^{C} \\ \boldsymbol{f}_2^{KE}(t)+\boldsymbol{f}_{1,2}^{C} \end{bmatrix}, \quad (5)$$

where the diagonal matrices $\boldsymbol{D}_j = \mathrm{diag}[2D_\nu^{(j)}\Omega_\nu^{(j)}]$, $j = 1, 2$ are determined by FA$_j$ eigenfrequencies $\Omega_\nu^{(j)}$ and damping factors $D_\nu^{(j)}$, $\nu = 1, \ldots, m_j$.

To perform dynamic analysis, the reduced model (5) is transformed to the state space

$$\dot{\boldsymbol{u}} = \boldsymbol{A}\boldsymbol{u} + \boldsymbol{f}(\boldsymbol{u}, t)\,. \quad (6)$$

The state vector $\boldsymbol{u}$ of dimension $2(m_1 + m_2)$ is defined as $\boldsymbol{u} = [\boldsymbol{x}_1^T, \boldsymbol{x}_2^T, \dot{\boldsymbol{x}}_1^T, \dot{\boldsymbol{x}}_2^T]^T$. The matrix $\boldsymbol{A}$ and the nonlinear vector $\boldsymbol{f}(\boldsymbol{u}, t)$ are defined as follows:

$$\boldsymbol{A} = -\begin{bmatrix} \mathbf{0} & \boldsymbol{I} \\ {}^m\boldsymbol{\Lambda} & \boldsymbol{D} \end{bmatrix}, \qquad \boldsymbol{f}(\boldsymbol{u}, t) = -\begin{bmatrix} \mathbf{0} \\ {}^m\boldsymbol{V}[\boldsymbol{f}_{KE}(t) + \boldsymbol{f}_C] \end{bmatrix}, \quad (7)$$

where $\boldsymbol{D}$, ${}^m\boldsymbol{\Lambda}$, ${}^m\boldsymbol{V}^T$, $\boldsymbol{f}_{KE}(t)$ and $\boldsymbol{f}_C$ are global matrices and vectors in (5). Model (6) is solved using a suitable numerical method in time-domain.

4. Application

To demonstrate the presented method, dynamic response of the statically deformed hexagonal FA$_1$ type 1 (eight spacer grids) and geometrically ideal hexagonal FA$_2$ type 2 (twelve spacer grids) in the MRC$_{132}$ (contains 132 FA$_2$ and 31 FA$_1$) was analysed. The FA$_1$ is statically deformed into a C-shape with forceless contact of both pairs of angles on the level of spacer grid $g = 5$ with the FA$_2$ between spacer grids 6 and 7 (see Fig. 2). The dynamic orbits of the FA$_1$ centre at the level of spacer grid $g = 5$ and the orbit of the FA$_2$ centre at the level of the spacer grid $g = 11$ are shown in Fig. 3. Dynamic orbits are shown for the FAs with the high fuel burn-up when gap between fuel pellets and FR cladding is closed. The orbits are depicted in a short time interval around extreme transverse FAs deformation.

Time-domain behaviour of normal contact forces $N_{1,2}$ ($N_{1,2} = N_{2,1}$) between FAs in time interval $t \in < 0; 5 >$[s] are shown in Fig. 4. Two states of both FAs were considered with the low (state I) and the high (state II) fuel burn-up. The normal forces in contact phases are larger in state II.

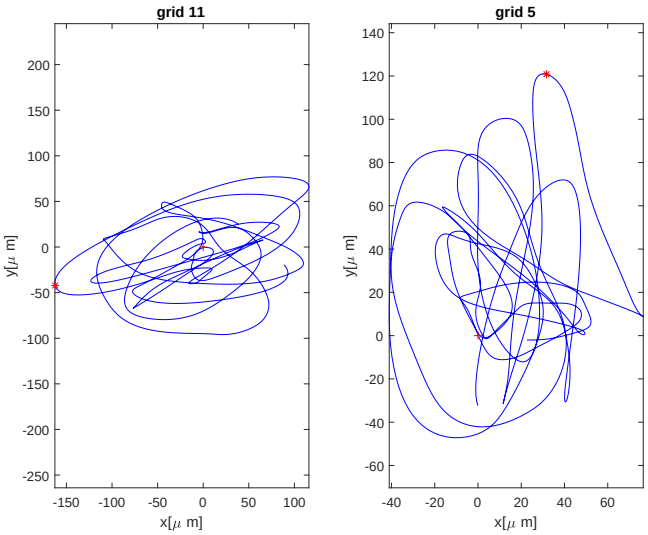

Fig. 3. Dynamic orbits of the FA_j's load bearing skeleton centre at the level of maximally deformed spacer grids

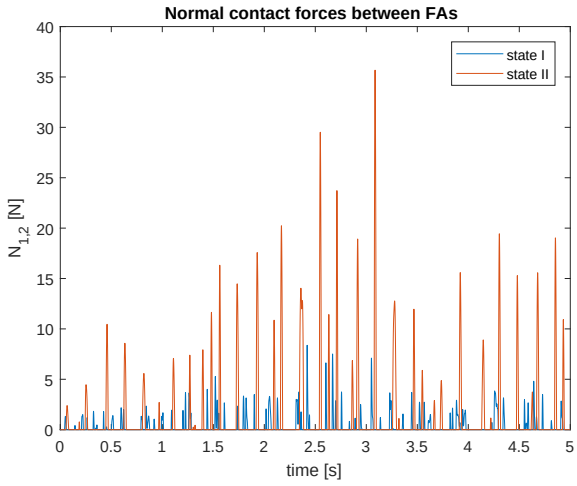

Fig. 4. Time-domain behaviour of the normal contact forces between FAs

Acknowledgement

This work was developed under the research project "Fuel Cycle of Nuclear Power Plant" coordinated by the Nuclear Research Institute Řež.

References

[1] Dyk, Š., Zeman, V., Hlaváč, Z., Mechanical interaction of bowed hexagonal fuel assemblies in PWR core, Progress in Nuclear Energy 161 (2023) No. 104732.

[2] Stulík, P. et al., Mechanical behaviour of the nuclear fuel, its monitoring and validation using operation measurement, Internal Research Report, Nuclear Research Institute Řež, 2020. (in Czech)

[3] Wanninger, A., Seidel, M., Macián-Juan, R., Mechanical analysis of the bow deformation of a row of fuel assemblies in PWR core, Nuclear Engineering and Technology 50 (2) (2018) 297-305.

[4] Zeman, V., Hlaváč, Z., Dynamic response of VVER 1000 type reactor excited by pressure pulsations, Engineering Mechanics 15 (6) (2008) 50-59.

[5] Zeman, V., Hlaváč, Z., Modelling of the friction-vibration interactions in reactor core barrel couplings, Applied and Computational Mechanics 12 (2) (2018) 193-212.